

Effect of the drainage layer on the thermal performance of green roofs in Curitiba-PR: comparative study with test cells ¹

Di Núbila Clarisse S.A.¹, Krüge Eduardo L.¹, Noya Mariana G.², González Cruz Eduardo M.¹

1. Federal University of Technology–Paraná (UTFPR) 2. Pontifical Catholic University of Paraná (PUC-PR)

Abstract: The present work aims to evaluate the effect of the material of the draining layer that constitutes a green roof system on its thermal behavior, considering the climate of Curitiba, by means of a comparative study using test cells. In order to do this, roof prototypes were constructed, which vary in terms of the material that constitutes the drainage layer: expanded clay, and two types of industrialized drainage blankets, one of which also has the function of storing water. This study analyzed the thermal performance of the green roof systems in terms of characteristic temperatures, time lag and decrement factor, resulting from the monitoring carried out in one week, in the end of summer (mar/2020). In the monitoring period, there was a slightly higher thermal performance of the green roof system whose drainage layer was composed of expanded clay.

Key words: green roof; drainage layer; thermal performance; test cells

1 Introduction

Studies have been conducted to evaluate the thermal performance of green roofs, both through measurements on full-scale roofs (PARIZOTTO; LAMBERTS, 2011; JIM; PENG, 2012; JIM, 2014; BUCKLAND-NICKS et al., 2016), as well as through prototypes (HINZ, 2006; LA ROCHE; BERARDI, 2014; ABREU et al., 2015; SAVI, 2015; LIZ et al., 2016; FEITOSA; WILKINSON, 2018; KAVISKI, 2018), in order to compare with other roofing systems, and also to study the influence of variations in certain parameters. However, few studies investigate the relationships between the drainage layer and the thermal performance of green roofs. Some of the existing studies focus on comparing traditional drainage systems with alternative drainage materials, such as shredded rubber (PÉREZ et al., 2012). Other studies, such as that by Scharf and Zluwa (2017), investigate different green roof systems by varying the material of the drainage layer, but simultaneously altering other components and characteristics of the system, making it difficult to analyze the influence of the drainage material alone on the thermal performance of the green roof.

In this context, the present study focuses on the use of test cells and green roof prototypes to evaluate the effect that changing the material of the drainage layer can have on the thermal performance of an extensive green roof in the climate of Curitiba. To this end, the characteristics of the system components are identical (plant species, materials, and layer thicknesses), with only the material of the drainage layer varying: expanded clay, drainage geomembrane, and drainage and water-retaining geomembrane.

2 Methodological procedures

This experimental and quantitative study was conducted using four test cells, referred to as modules, consisting of one control module (CM) and three experimental modules (EMs). Green roof prototypes were installed on each of the EMs.

2.1 Experiment site

The experiment was conducted at the Experimental Site of the Graduate Program in Civil Engineering (PPGEC) at the Federal Technological University of Paraná (UTFPR), Curitiba Campus, Ecoville headquarters. The university is located at an elevation of 950 m, with geographical coordinates of approximately 25.44°S, 49.35°W (DSG, 2020). The city of Curitiba (PR) is situated in Bioclimatic Zone 1, with a humid maritime temperate climate (Cfb), according to the Köppen-Geiger classification.

2.2 Green roof prototypes

The green roof prototypes were constructed from 15-mm-thick marine plywood, painted with water-based white enamel paint (3 coats), and lined on the sides (inner surface) with 60-mm expanded polystyrene (EPS). The waterproofing layer, applied internally, consists of polymer mortar (3 coats) and polyester mesh. On one side of the prototype there is a 2.5 x 34 cm opening through which drained water flows. The external dimensions of the prototypes are 49.5 x 49.5 cm, and the internal dimensions are 34 x 34 cm each (excluding the thickness of the mortar).

The study focuses on three extensive green roof systems: ARG, GD, and GDA. The ARG type features a drainage layer composed of type 2215 expanded clay (fine-grained), which forms a 4 cm thick layer. A filter layer, composed of a nonwoven geotextile, was placed over the expanded clay. Regarding the GD type, the drainage layer consists of a structured drainage geocomposite (MacDrain® 1L) formed by polypropylene filaments that make up a flexible three-dimensional geomanta, which has 90% voids, bonded to a nonwoven geotextile. It is approximately 1 cm thick, and its drainage capacity is 144 L/h. This geocomposite already serves a filtering function, so no additional layer is required. The GDA type, on the other hand, features a drainage layer composed of an extruded high-density polyethylene (HDPE) membrane, which, in addition to its drainage function, also serves as a water storage layer (Maxistud®). The water storage capacity of this membrane is 3.6 L/m², its height is 2 cm, and the thickness of the HDPE film is 1.05 mm. The water stored in this system is subsequently released into the substrate through evaporation. A structured geotextile (HDPE weave) with nonwoven geotextile on one side was placed over this drainage and water-storage geomembrane to form the filtration layer.

The remaining layers (substrate and plant layer) are identical in all systems. The substrate layer is 15 cm thick and consists of a commercial substrate and 10% by weight of medium-grained sand. The substrate consists of soil, rice husks, pine bark, and slow-release fertilizer. The sand added to the substrate is sold by a building materials store. The materials were mixed and placed in the prototypes with their original moisture content. A layer of shredded pine bark was spread over the substrate layer for protection. The plants used in the green roof are of the species *Bulbine frutescens* (bulbine), a perennial herbaceous plant, generally grown in full sun, and undemanding in terms of water (succulent plant) (LORENZI, 2015), making it suitable for green roofs. Native to South Africa, this herbaceous plant is cold-tolerant (LORENZI, 2015), making it suitable for the climate of Curitiba. Planting took place in the summer, on December 4, 2019, with 5 seedlings per prototype. The degree of vegetation cover of the prototypes during the monitoring period was 74% for the ARG prototype and 70% for the GD and GDA types, considering only the foliage and disregarding the projection of inflorescences and stems.

2.4 Experimental modules and control

The test cells (modules) used in this study were constructed based on cells developed by González (1997), but with reduced dimensions. The modules are made of 15 mm thick marine plywood sheets, painted with water-based white enamel paint (3 coats), and lined internally with 45 mm of EPS (sides and bottom). The modules have rubber supports,

which ensure a 2% slope in the case of the MEs. The control module (CM) measures 46 x 46 x 25.5 cm and has a lid lined with special thermal insulation ($U=0.36 \text{ W/m}^2\text{K}$), consisting of 100 mm of EPS, to minimize heat gain through the top surface, giving the CM a total height of 32 cm. The experimental modules (EMs), in turn, have external dimensions of 46 x 46 x 20.5 cm. The upper part of the EMs consists of the vegetation cover prototypes: EM1 (ARG-type prototype); EM2 (type GD); ME3 (GDA-type prototype). The internal volume is the same for the MEs and MCs, measuring 34 x 34 x 14.5 cm.

2.5 Data acquisition and sensor placement

Monitoring of the prototypes was conducted from March 11 to March 18, 2020, at the end of summer. Table 1 lists the equipment used in the experiment, which was programmed to collect data every 5 minutes, while Figure 1 schematically illustrates their positions.

Table 1. Equipment/sensors used in the experiment. Source: the authors

Symbol	Equipment	Variables	Quantity	Position
◆	Sensor S-THB-002 Onset*	Outdoor air temperature (°C) and relative humidity (RH, %)	1	1.75 m above floor level, inside a meteorological shelter
×	Rain gauge RGF-M002 Davis*	Precipitation (mm)	1	1.85 m above floor level
■	Datalogger LogBox-RHT Novus	Indoor air temperature (°C) and relative humidity (RH, %)	4	At the center of the experimental and control modules
●	Datalogger TagTemp NFC Novus	Surface temperature (°C) Substrate temperature (°C)	3 3	Underside of the prototypes At the midpoint of the substrate layer
▲	Sensor S-SMC-M005 Onset*	Volumetric water content of the substrate (% vol.)	3	At the midpoint of the substrate layer

*connected to the Onset Hobo U12-001 Station (data logger)

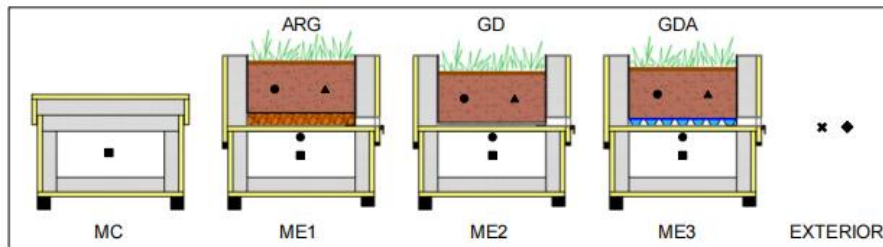


Figure 1. Diagram of sensor placement (cross-section). Source: the authors

The LogBox RHT and TagTemp NFC temperature sensors underwent a calibration process against a sensor with a calibration certificate, model Hobo UX100-023 Onset, which measures air temperature and RH. Correction equations were determined for each of the sensors relative to the reference sensor (Hobo UX100-023).

2.6 Thermal performance-evaluated parameters

To analyze the thermal performance of the systems, characteristic temperatures, thermal lag, and the decrement factor were evaluated. The characteristic temperatures correspond to the maximum (T_{max}), minimum (T_{min}), and average (T_{med}) temperature values, measured inside the experimental and control modules, and in the external environment. Thermal lag is calculated as the amount of time (h) it takes for the daily temperature variation to elapse and manifest on the internal surface of the experimental modules. The higher the thermal lag, the higher the thermal inertia of the system (FROTA; SCHIFFER, 2001). The decrement factor represents the degree of thermal damping of the indoor environment with respect to outdoor temperature variations, and is expressed as the ratio of the daily temperature range of the indoor air

to that of the outdoor air. The lower the DF, the greater the capacity to reduce the variation in indoor temperature relative to the outdoors (KRÜGER et al., 2010), indicating better thermal performance.

3 Results

Figure 2 presents a graph showing the indoor air and surface temperatures of the modules, as well as the outdoor air temperature and relative humidity, for the period from March 11 to 18, 2020. During this period, the outdoor temperature ranged from 14.3°C to 32.1°C, and the RH from 29% to 94%. Throughout the monitoring period, precipitation events were recorded on March 16 and 18, measuring 3.2 mm and 5.6 mm, respectively.

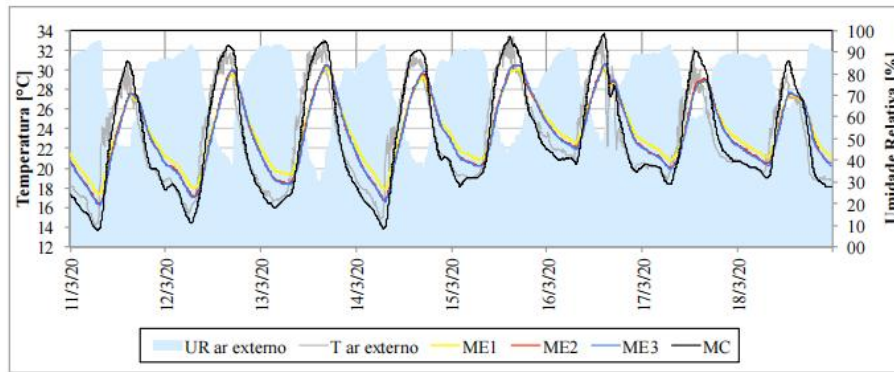


Figure 2. Indoor air temperatures in the modules, and outdoor air temperature and RH (March 11–18, 2020). Source: the authors

Figure 3 shows the maximum, average, and minimum indoor air temperatures of the modules and the outdoor environment for each of the 8 days of monitoring. It can be seen that, in all experimental modules, the green roof systems contributed to a reduction in maximum temperatures compared to the outdoors and the control module. Compared to the outdoor temperature, this reduction reached 2.1 °C in the case of ME1, and 1.7 °C in the case of ME2 and ME3. Regarding average air temperatures, it was found that, inside the experimental modules, these reached values equal to or higher than those in the outdoor environment. The mean air temperature (Tmed) inside ME1 was on average 0.8 °C higher than outside, while this difference was on average 0.4 °C and 0.3 °C for ME2 and ME3, respectively. When comparing minimum temperatures, ME1 showed an average increase of 2.4°C compared to the external environment, and 1.6°C and 1.5°C for ME2 and ME3, respectively.

It can therefore be concluded that the systems evaluated are capable of reducing the maximum indoor air temperature compared to the outdoor environment and the MC; in all experiments, minimum temperatures higher than those of the outdoor environment and the MC were obtained; consequently, a slight increase in the average temperature of the MEs is observed compared to the outdoors and the MC. When comparing the MEs among themselves, it is found that the ME2 and the ME3 exhibit similar thermal behavior, while the temperature differences between ME1 and the others are on average -0.3° C for Tmax, +0.4 ° C for Tmed, and +0.9 ° C for Tmin.

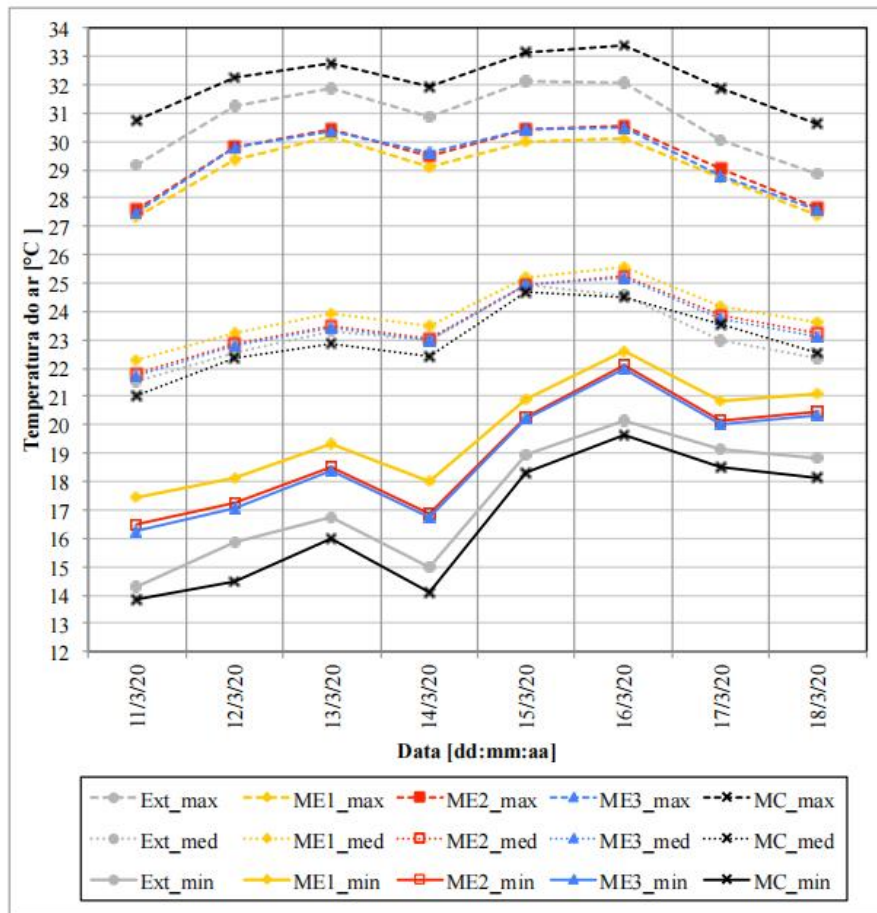


Figure 3. Maximum, average, and minimum indoor air temperatures of the modules and outdoor air. Source: the authors

The graph in Figure 4 shows the temperature and volumetric water content (VWC) of the substrate. It can be observed that the substrate temperature of module ME1 exhibits a slightly smaller amplitude than modules ME2 and ME3, which show a similar variation in temperature over time. This may explain the observed reduction in the thermal amplitude of the internal air in module ME1 (ARG prototype, with expanded clay). The substrate in the MEs remained dry throughout virtually the entire period, with VWC between 0.10 and 0.15 m³/m³, which rose only on March 18 due to a rain event. It can be observed that, due to the precipitation, the CVA values were lower in ME2 and higher in ME3, indicating better drainage capacity for the green roof with GD, and worse in the case of the roof with GDA.

Table 2 presents the thermal lag values, as well as the decrement factors. For this analysis, hourly average temperatures were considered for each day (for thermal lag, the internal surface temperature was considered).

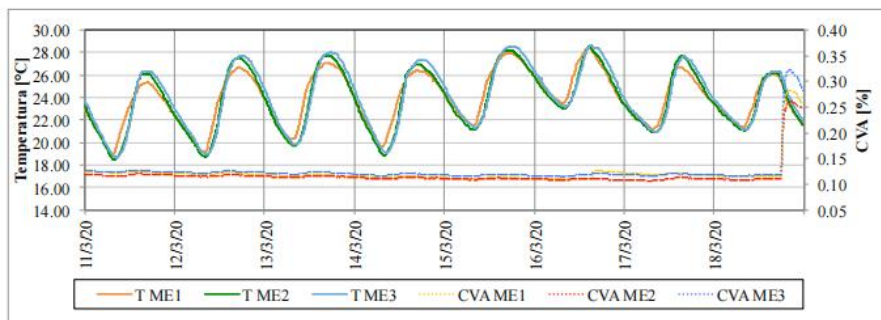


Figure 4. Substrate temperature and volumetric water content. Source: the authors

Table 2. Thermal lag of the green roof prototypes and temperature reduction factors for the experimental and control modules. Source: the authors

DATE	Thermal Lag (hours)			Decremental Factor			
	ME1	ME2	ME3	ME1	ME2	ME3	MC
11/3/20	2	2	2	0.66	0.75	0.75	1.13
12/3/20	2	2	2	0.73	0.82	0.83	1.16
13/3/20	1	1	1	0.71	0.79	0.79	1.11
14/3/20	3	3	3	0.70	0.79	0.81	1.12
15/3/20	3	3	3	0.69	0.77	0.78	1.13
16/3/20	1	1	1	0.63	0.71	0.71	1.15
17/3/20	3	3	3	0.72	0.81	0.80	1.22
18/3/20	3	2	3	0.63	0.71	0.72	1.25
Average	2.3	2.1	2.3	0.69	0.77	0.78	1.16

It is observed that the thermal lag provided by the prototypes varies between 1 and 3 hours over the monitoring period. The pattern of variation in the thermal delay of the prototypes remains consistent on most days. Upon analyzing the decrement factor of the modules, it is observed that lower values are obtained by ME1, indicating a greater capacity to reduce internal temperature variation.

4 Conclusion

It is concluded that the prototype with expanded clay in the drainage layer (ARG) exhibits slightly better thermal performance compared to the prototypes with a drainage geomembrane (GD) and a drainage and water-retaining geomembrane (GDA) during the period analyzed. It should be noted that the CVA of the prototypes indicated that the substrate was dry. In the future, analyses will be conducted under different weather conditions in Curitiba to verify whether this behavior pattern varies depending on these conditions.

Acknowledgments

The authors thank Capes, UTFPR, Prof. Massayuki Mário Hara, Paulo Sabino, Ângela Deeke Sasse, Endrio Lázaro de Freitas Nascimento, and the companies Diprotec and Maccaferri.

Conflicts of interest

The author declares no conflicts of interest regarding the publication of this paper.

References

- [1] ABREU, A. L. P.; GOES, F.; BAUMANN, V. A. R. Protótipos parciais de cobertura verde para estudo da redução da carga térmica interna de edificação escolar em Florianópolis. In: XIII Encontro Nacional e IX Encontro Latino-americano de Conforto no Ambiente Construído. Anais... Campinas: ENCAC/ELACAC. 2015.
- [2] BUCKLAND-NICKS, M.; HEIM, A.; LUNDHOLM, J. Spatial environmental heterogeneity affects plant growth and thermal performance on a green roof. *Science of the Total Environment*, v. 553, p. 20–31, 2016.
- [3] DSG - Diretoria de Serviço Geográfico. Banco de Dados Geográficos do Exército (BDGEx). 2020. Disponível em: .Acesso em: 11 fev. 2020.
- [4] FEITOSA, R. C.; WILKINSON, S. J. Attenuating heat stress through green roof and green wall retrofit. *Building and Environment*, v. 140, p. 11–22, 2018.
- [5] FROTA, A. B.; SCHIFFER, S. R. Manual de conforto térmico. 5 ed. São Paulo: Studio Nobel, 2001.

[6] GONZÁLEZ, E. M. Étude de Matériaux et de Techniques du Bâtiment Pour la Conception Architecturale Bioclimatique en Climat Chaud et Humide. Tese (Doutorado)– l'École des Mines des Paris. Paris, 1997.

[7] HINZ, E. Estudio del comportamiento térmico de un sistema pasivo de enfriamiento evaporativo indirecto con cobertura vegetal en un clima tropical. Tese (Doutorado em Ciências Ambientais)- Universidade de Zulia, Maracaibo, 2006.

[8] JIM, C.Y. Passive warming of indoor space induced by tropical green roof in winter. *Energy*, v. 68, p.272–282, 2014.

[9] JIM, C.Y.; PENG, L. L. H. Substrate moisture effect on water balance and thermal regime of a tropical extensive green roof. *Ecological Engineering*, v.47, p. 9–23, oct. 2012.

[10] KAVISKI, F. Desempenho térmico de cobertura vegetada sobre guarita de fibra de vidro exposta a diferentes condições climáticas em Curitiba. Dissertação (Mestrado), Programa de Pós-graduação em Engenharia Civil, Universidade Tecnológica Federal do Paraná, Curitiba, 2018.

[11] KR ÜGER, E.; GONZÁLEZ CRUZ, E.; GIVONI, B. Effectiveness of indirect evaporative cooling and thermal mass in a hot arid climate. *Building and Environment*, v.45, p. 1422–1433, 2010.

[12] LA ROCHE, P.; BERARDI, U. Comfort and energy savings with active green roofs. *Energy and Buildings*, v.82, p.492–504, 2014.

[13] LIZ, D. G.S. de; MIZGIER, M. O.; GÜTHS, S. Análise experimental do comportamento térmico do telhado verde extensivo para Florianópolis. In: ENCONTRO NACIONAL DE TECNOLOGIA DO AMBIENTE CONSTRUÍDO, 16., 2016, São Paulo. Anais... Porto Alegre: ANTAC, 2016.

[14] LORENZI, H. Plantas para jardim no Brasil: herbáceas, arbustivas e trepadeiras. 2 ed. Nova Odessa: Instituto Plantarum, 2015.

[15] PARIZOTTO, S.; LAMBERTS, R. Investigation of Green Roof Performance in Temperature Climate: A Case Study of an Experimental Building in Florianópolis City, Southern Brazil. *Journal of Energy and Buildings*, Amsterdam, v.43, p.1712- 1722, 2011.

[16] PÉREZ, G.; VILA, A.; RINCÓN, L.; SOLÉ, C.; CABEZA, L. F. Green roofs as passive system for energy savings when using rubber crumbs as drainage layer. *Energy Procedia*, v.30, p.452-460, 2012.

[17] SAVI, A. C. Telhados Verdes: uma análise da influência das espécies vegetais no seu desempenho na cidade de Curitiba. 2015. Dissertação (Mestrado), Programa de Pós-graduação em Engenharia de Construção Civil, Universidade Federal do Paraná, Curitiba, 2015.

[18] SCHARF, B.; ZLUWA, I. Case study investigation of the building physical properties of seven different green roof systems. *Energy and Buildings*, v. 151, p.564–573, jun. 2017.

Note

¹ DI NÚBILA, Clarisse S.A.; KRÜGER, Eduardo L.; NOYA, Mariana G.; GONZÁLEZ CRUZ, Eduardo M. Effect of the drainage layer on the thermal performance of green roofs in Curitiba-PR: Comparative study with test cells. In: NATIONAL MEETING ON BUILDING ENVIRONMENT TECHNOLOGY, 18th, 2020, Porto Alegre. Proceedings... Porto Alegre: ANTAC, 2020.